

Enhancement of magnetic surface anisotropy of Pd/Co/Pd trilayers by the addition of Sm

著者	北上 修
journal or publication title	Journal of Applied Physics
volume	90
number	8
page range	4085-4088
year	2001
URL	http://hdl.handle.net/10097/47662

doi: 10.1063/1.1405817

Enhancement of magnetic surface anisotropy of Pd/Co/Pd trilayers by the addition of Sm

Satoshi Okamoto,^{a)} Katsuya Nishiyama, Osamu Kitakami, and Yutaka Shimada
Research Institute for Scientific Measurements, Tohoku University, Sendai 980-8577, Japan

(Received 9 April 2001; accepted for publication 27 July 2001)

We have studied the effect of Sm on the magnetic surface anisotropy (MSA) of Pd/Co_{100-x}Sm_x/Pd (111) trilayers, where Sm content x was varied from 0 to 11. All samples show perpendicular anisotropy due to the strong MSA at the interfaces. The MSA significantly increases with x and attains a maximum value of 0.60 erg/cm² at $x \approx 8.3$, which is 36% larger than that of pure Co ($x=0$). The volume term of the magnetic anisotropy shows a similar behavior as the MSA. The appreciable increase in MSA is considered to be due to the enhancement of orbital moment of Co by the addition of Sm. © 2001 American Institute of Physics. [DOI: 10.1063/1.1405817]

I. INTRODUCTION

In the last decade intensive studies have been devoted to Co/Pt and Co/Pd multilayers because they exhibit large Kerr rotation and strong perpendicular magnetic anisotropy. Such large magnetic anisotropy is attributed to the magnetic surface anisotropy (MSA) at the interfaces.¹ The MSA at the interface of a $3d/5d$ transition metal system originates from enhanced spin-orbit coupling of $3d$ transition metal through an electronic coupling with $5d$ transition metal.² Keavney *et al.* found that several rare earth (RE) elements in Co significantly enhance the ratio of orbital to spin moment of Co, and insisted that the large orbital moment of Co enhances the magnetocrystalline anisotropy (MCA).³ They also found that the ratio took a maximum for RE=Sm, and the ratio is almost four times larger than that for pure Co. The large orbital moment of Co in Co-Sm is expected to enhance the MSA as well as the MCA.

In this article we study the magnetic anisotropy of Pd/Co-Sm/Pd trilayers and demonstrate that Sm considerably enhances the MSA of Co.

II. EXPERIMENT

Pd (50 Å)/Co_{100-x}Sm_x (d Å)/Pd (200 Å) trilayers ($x=0-11$) were prepared on HF treated Si (001) by dc magnetron sputtering at room temperature. The Co-Sm thickness d was varied from 2 to 300 Å. The sputtering chamber was evacuated up to 3×10^{-8} Torr prior to film deposition, Ar gas pressure was kept at 2 mTorr during sputtering. The deposition rates for Co-Sm and Pd were 2.6–3.3 and 26 Å/min, respectively. Film thickness was determined from x-ray reflectivity measurements with an accuracy of 1%. The film compositions were determined by x-ray photoelectron spectroscopy (XPS). The crystal structures were investigated by reflection high-energy electron diffraction (RHEED) and conventional x-ray diffraction. The magnetization was measured by using a vibrating sample magnetometer (VSM) with a maximum field of 15 kOe and the perpendicular magnetic

anisotropy at room temperature was determined by magneto-optical Kerr effect (MOKE) with a maximum field of 7.8 kOe.

III. DETERMINATION OF PERPENDICULAR MAGNETIC ANISOTROPY

For magnetic anisotropy measurements we used the MOKE system with a configuration similar to that reported by Purcell *et al.*⁴ (Fig. 1). The angle θ_H of the external field H from the film normal was fixed at 85°, 80°, and 70°. By tilting the sample plane slightly with respect to the external field, magnetization proceeds by coherent rotation, because nucleation of reversed magnetic domains can be suppressed by the presence of the field component along the film normal. The Kerr ellipticity curves were measured at various θ_H , as shown in Fig. 2(a). The total magnetic energy is given by

$$E = K_1^{\text{eff}} \sin^2 \theta_M + K_2 \sin^4 \theta_M - M_S H \cos(\theta_M - \theta_H), \quad (1)$$

$$K_1^{\text{eff}} = K_{V1}^{\text{eff}} + 2K_{S1}/d, \quad (2)$$

$$K_2 = K_{V2} + 2K_{S2}/d, \quad (3)$$

where θ_M denotes the angle of the magnetization from the film normal, M_S is the saturation magnetization, K_{V1}^{eff} and K_{V2} are the first and the second order volume anisotropy constants, and K_{S1} and K_{S2} are the first and the second order surface anisotropy constants, respectively. The K_{V1}^{eff} includes both the intrinsic volume anisotropy K_{V1} and the demagnetizing energy $2\pi M_S^2$. From Eq. (1) the equilibrium condition is given by

$$(K_1^{\text{eff}} + K_2 \sin^2 \theta_M) \sin 2\theta_M + M_S H \sin(\theta_M - \theta_H) = 0. \quad (4)$$

Purcell *et al.*⁴ evaluated the anisotropy constants of Co/Pd multilayers by numerical fitting of Eq. (4) with the field dependence of normalized Kerr ellipticity ($\cos \theta_M$) shown in Fig. 2(a). However, a small variation of Kerr ellipticity makes it difficult to accurately evaluate the anisotropy constants when the magnetic anisotropy is very strong. In fact, they reported that accurate determination of K_2 was difficult

^{a)}Corresponding author; electronic mail: okamotos@rism.tohoku.ac.jp

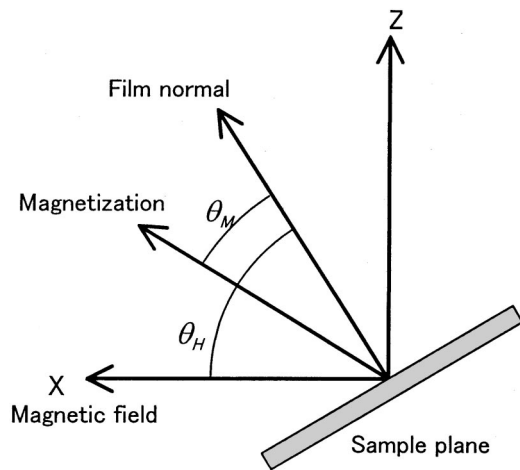


FIG. 1. Illustration of the MOKE measurement system. The plane of incidence is orthogonal to the x - z plane.

for $K_1^{\text{eff}} > 5 \times 10^6 \text{ erg/cm}^3$. In order to avoid this problem we derived the following equilibrium equation from Eq. (4);

$$\frac{2K_1^{\text{eff}}}{M_S} + \frac{4K_2}{M_S}(1 - m^2) = \alpha H, \quad (5)$$

where

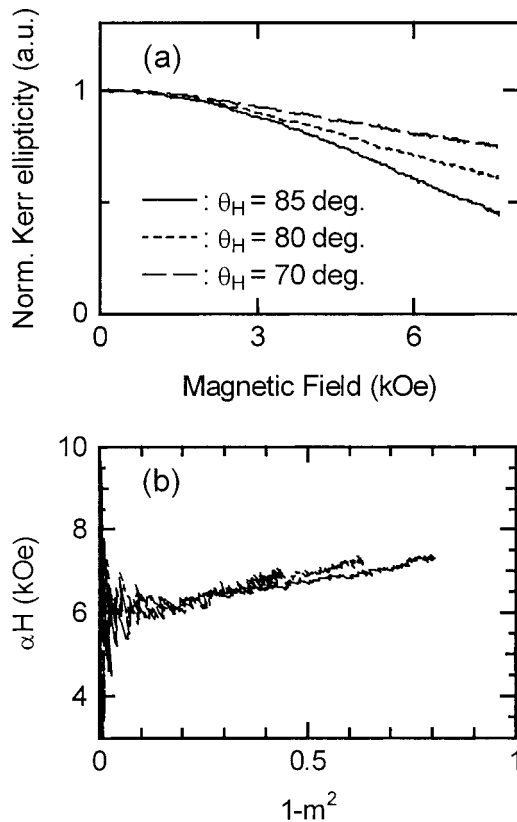
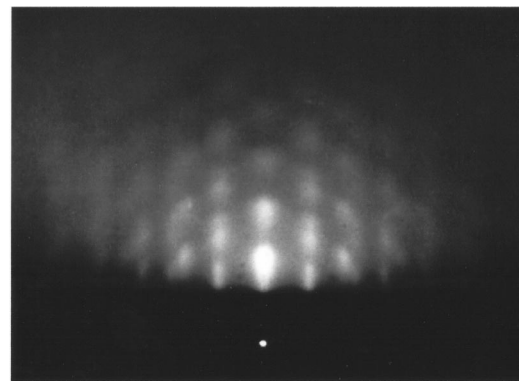
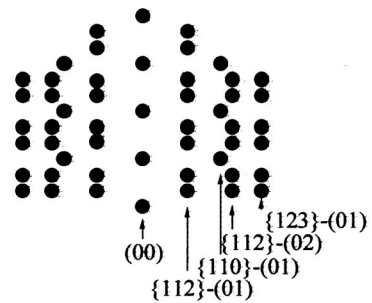


FIG. 2. (a) Normalized Kerr ellipticity vs magnetic field for Pd (50 Å)/Co (5.4 Å)/Pd (200 Å) measured at $\theta_H = 85^\circ, 80^\circ,$ and 70° . (b) αH vs $(1 - m^2)$. The ellipticity curves in (a) are replotted using the equilibrium relation Eq. (5).



(a)



(b)

FIG. 3. (a) RHEED pattern of the 200-Å-thick Pd layer. (b) Reciprocal spots of 2D random fcc (111) orientation. $\{hkl\}-(mn)$ in (b) indicates the reciprocal rod (mn) from the $\{hkl\}$ plane which is orthogonal to (111) plane.

$$\alpha = \frac{m \sin \theta_H - \sqrt{1 - m^2} \cos \theta_H}{m \sqrt{1 - m^2}}$$

and $m = \cos \theta_M$. For $\theta_H = 90^\circ$, Eq. (5) coincides with the well-known Sucksmith–Tompson’s relation.⁵ By taking the right term of Eq. (5) as the vertical axis and $(1 - m^2)$ as the horizontal axis, the MOKE curves in Fig. 2(a) can be replotted as shown in Fig. 2(b). Note that all three curves in Fig. 2(a) fall in one straight line, indicating that magnetization proceeds through coherent rotation. From this intersection and slope we can determine K_1^{eff}/M_S and K_2/M_S . The three straight lines in Fig. 2(b) do not completely coincide with each other, which is probably due to a setting error of θ_H , resulting in a measurement error of K_1^{eff} and K_2 . For the present Pd/Co_{100-x}Sm_x/Pd, the measurement error of K_1^{eff} was less than $\pm 5\%$, as will be mentioned later.

IV. RESULTS AND DISCUSSION

Figure 3(a) shows the RHEED pattern of the 200-Å-thick Pd layer grown on Si. The spotty diffractions indicate that the Pd surface is somewhat rough. All these diffraction spots are assigned to the reciprocal lattice of two-dimensional (2D) randomly oriented fcc (111) [Fig. 3(b)]. X-ray diffractions also showed perfect orientation of Pd (111). Co_{100-x}Sm_x (111) were epitaxially grown on Pd (111). As the Sm content x increases above 8 at. %, RHEED diffraction spots gradually diminished, indicating that the film tends to become amorphous.

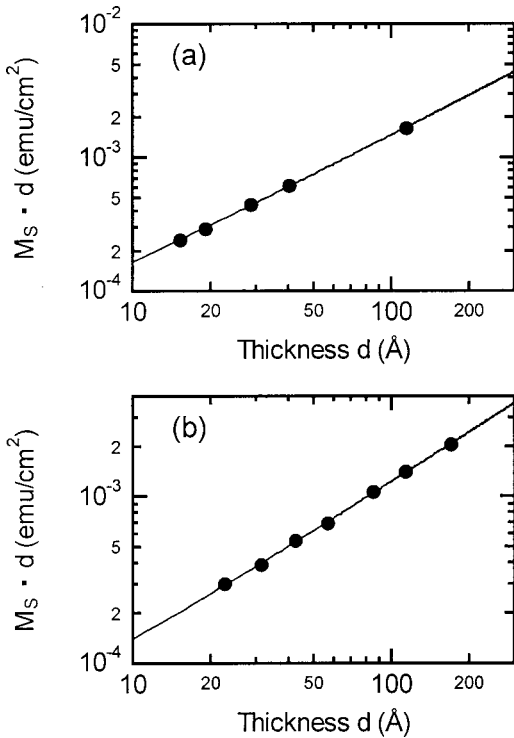


FIG. 4. $M_S \cdot d$ vs thickness d for (a) Pd(50 Å)/Co(d Å)/Pd(200 Å) and (b) Pd(50 Å)/Co_{91.7}Sm_{8.3}(d Å)/Pd(200 Å). Solid lines are the best fit.

In general, magnetization $M_S \cdot d$ (d is the magnetic layer thickness) would be expressed as

$$M_S \cdot d = M_V \cdot d + \Delta M, \quad (6)$$

where M_V is the volume magnetization and ΔM denotes the surface magnetization induced by polarization of Pd and/or enhanced Co moment at the interfaces. Figures 4(a) and 4(b) show $M_S \cdot d$ vs d plots for Pd/Co/Pd and Pd/Co_{91.7}Sm_{8.3}/Pd, respectively. Note that all data points in Fig. 4 perfectly follow the relationship of Eq. (6) with an error less than 5%, allowing accurate determination of M_V and ΔM . For Pd/Co/Pd, M_V is determined as 1450 ± 20 emu/cm³, which agrees with the value of bulk Co (1420 emu/cm³) within the experimental error. ΔM is 2.0×10^{-5} emu/cm², again in good agreement with the value reported by Engel *et al.*⁶ The induced moment per Pd atom at the interface is estimated to be $0.82\mu_B$, which is nearly equal to the total induced moment ($0.66\mu_B$) predicted by the band calculation for Co/Pd.² For more quantitative discussion, ΔM should be measured at $T \sim 0$ K because the band calculation gives the value at 0 K. Figure 5 shows M_V and ΔM as a function of Sm content x . M_V monotonically decreases with x , while ΔM remains constant within the experimental error. Very little change in ΔM against x suggests that the induced interfacial moment ΔM comes from the polarization of Pd atoms at the interface.

Figures 6(a) and 6(b), respectively, show $K_1^{\text{eff}} \cdot d$ and $K_2 \cdot d$ for the Pd/Co/Pd and Pd/Co_{91.7}Sm_{8.3}/Pd as functions of d . Both $K_1^{\text{eff}} \cdot d$ and $K_2 \cdot d$ linearly decrease with increasing d . Using Eqs. (2) and (3), K_{V1}^{eff} , K_{V2} , K_{S1} , and K_{S2} can be evaluated as $K_{S1} = 0.42 \pm 0.02$ erg/cm², $K_{S2} = 0.03 \pm 0.02$ erg/cm² for Pd/Co/Pd, and $K_{S1} = 0.57 \pm 0.03$ erg/cm², $K_{S2} = 0.03 \pm 0.02$ erg/cm² for Pd/Co_{91.7}Sm_{8.3}/Pd. The obvi-

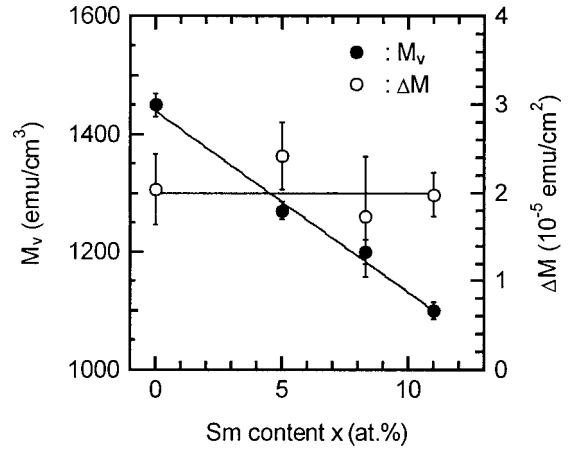


FIG. 5. Variation of M_V and ΔM for Pd(50 Å)/Co_{100-x}Sm_x (12–300 Å)/Pd (200 Å) as a function of Sm content x . Solid lines are guides to the eye.

ous deviation of $K_i \cdot d$ from the linear relation in the very thin region ($d < 3$ Å) may be related to the incomplete layer structure, which tends to be island-like. Figure 7 shows the variation of $K_S (= K_{S1} + K_{S2})$ as a function of x . Since K_{S2} is much smaller than K_{S1} , the behavior of K_S in Fig. 7 is exclusively dominated by K_{S1} . Furthermore, it should be noted that K_S rapidly increases with x up to 8.3 at.%, and then decreases. The decrease in K_S for $x > 8.3$ may be related to the degradation of the Co–Sm crystal structure, as mentioned before. K_S attains a maximum value of 0.60 ± 0.03 erg/cm² at $x \sim 8$, which is 36% larger than that for pure Co. In Fig. 8 the effective volume anisotropy K_{V1}^{eff}

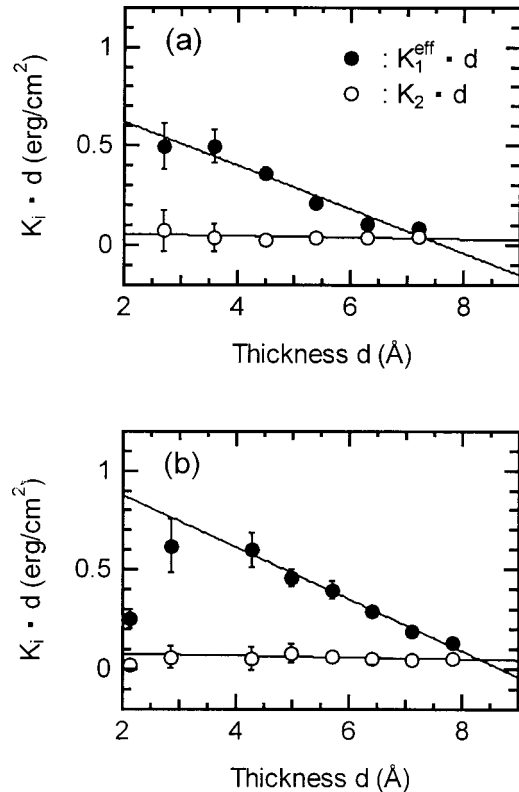


FIG. 6. $K_1^{\text{eff}} \cdot d$ and $K_2 \cdot d$ vs d for (a) Pd(50 Å)/Co(d Å)/Pd(200 Å) and (b) Pd(50 Å)/Co_{91.7}Sm_{8.3}(d Å)/Pd(200 Å). Solid lines are the best fit.

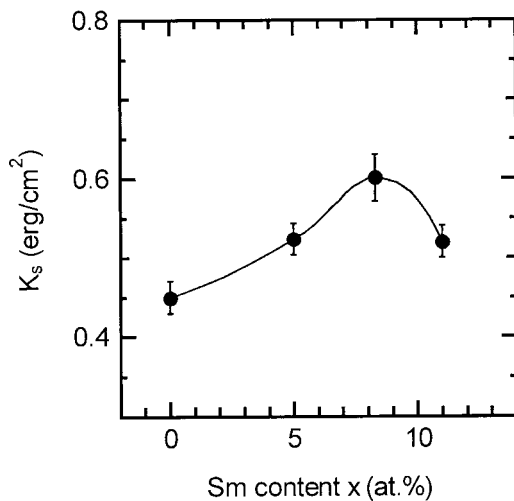


FIG. 7. Surface anisotropy K_S vs Sm content x for Pd(50 Å)/Co_{100-x}Sm_x (2–10 Å)/Pd (200 Å).

($=K_{V1}-2\pi M_S^2$) and the demagnetization energy $-2\pi M_S^2$ are plotted as functions of the Sm content x . The $-2\pi M_S^2$ monotonically decreases with x , while K_{V1}^{eff} gradually increases up to $x \sim 8$ and then drastically decreases. Since the difference between K_{V1}^{eff} and $-2\pi M_S^2$ corresponds to K_{V1} , the intrinsic volume anisotropy is obviously enhanced by Sm for $x \leq 8$. This behavior looks very similar to that of K_S in Fig. 7 although their signs are opposite.

Let us discuss the significant enhancement of the MSA due to Sm. In addition to the broken symmetry at the interfaces, magnetoelastic effect due to the lattice misfit at the interface is likely to make an appreciable contribution to MSA. However, the magnetostriction coefficient λ for poly-

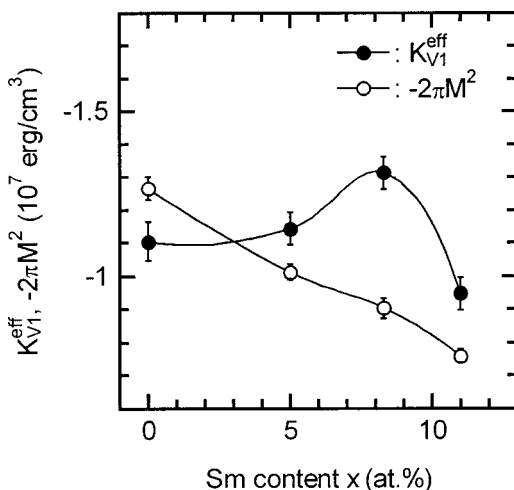


FIG. 8. Volume anisotropy K_{V1}^{eff} and $2\pi M_S^2$ vs Sm content x for Pd(50 Å)/Co_{100-x}Sm_x/Pd (200 Å).

crystalline Co_{100-x}Sm_x ($x=11-33$) is reported to be nearly zero,⁷ and therefore magnetoelastic contribution to the MSA can be neglected. Very little magnetoelastic effect is supported for the following reasons. At the initial growth stage, a Co layer is coherently strained due to the lattice misfit with Pd, and at a certain critical thickness d_{crit} the stress is abruptly released by introducing dislocations.¹ Therefore if the MSA of Pd/Co/Pd is mainly dominated by the magnetoelastic effect, $K_i \cdot d$ must exhibit a sudden change against d at d_{crit} where the coherent strain is released. As can be noticed in Fig. 6(a), $K_i \cdot d (=V_V \cdot d + 2K_S)$ obeys a linear relationship and no sudden changes can be seen. Recently, Keavney *et al.* measured the orbital moment of Co in several Co-RE alloys using the x-ray magnetic circular dichroism.³ They clarified the close relationship between the Co orbital moment and the Co-RE bond length, and found a very large orbital moment of Co in Co-Sm. This finding leads us to think that the significant increase of MSA by the addition of Sm should be attributed to the spin-orbit coupling enhanced by Sm.

V. CONCLUSIONS

We have studied the effect of a Sm additive on the magnetic properties of Pd/Co_{1-x}Sm_x/Pd trilayers ($0 \leq x \leq 11$). The Co-Sm/Pd interface exhibits an induced magnetic moment of $\sim 2 \times 10^{-5}$ emu/cm² ($\sim 0.8\mu_B$ /Pd atom) for the whole Sm content examined in the present study. Moreover, Sm significantly enhances the magnetic surface anisotropy K_S . The maximum K_S reaches is 0.60 ± 0.03 erg/cm² at $x \sim 8$ at.%, which is 36% larger than that for pure Co. For further increase of x K_S decreases due to the degradation of crystal quality. Such a remarkable increase in the surface anisotropy may be attributed to the strong spin-orbit coupling by a Co orbital moment enhanced in Co-Sm.

ACKNOWLEDGMENTS

This work was supported by the Research for the Future Program of Japan for the Promotion of Science under Grant No. 97R14701, and the Storage Research Consortium in Japan.

¹M. T. Johnson, R. Jungblut, P. J. Kelly, and F. J. A. den Broeder, *J. Magn. Magn. Mater.* **148**, 118 (1995).

²K. Kyuno, J. G. Ha, R. Yamamoto, and S. Asano, *Phys. Rev. B* **54**, 1092 (1995).

³D. J. Keavney, E. E. Fullerton, D. Li, C. H. Sowers, and S. D. Bader, *Phys. Rev. B* **57**, 5291 (1998).

⁴S. T. Purcell, M. T. Johnson, N. W. E. McGee, W. B. Zeper, and W. Hoving, *J. Magn. Magn. Mater.* **113**, 257 (1992).

⁵W. Sucksmith and J. E. Thompson, *Proc. R. Soc. London, Ser. A* **225**, 362 (1954).

⁶B. N. Engel, C. D. England, R. V. Leeuwen, M. Nakada, and C. M. Falco, *J. Appl. Phys.* **69**, 5643 (1991).

⁷S. Ishio, M. Takahashi, and T. Miyazaki, *J. Magn. Magn. Mater.* **86**, 31 (1990).